Spectrochimica Acta Part A 88 (2012) 31–36

Contents lists available at SciVerse ScienceDirect

Spectrochimica Acta Part A: Molecular and Biomolecular Spectroscopy

journal homepage: www.elsevier.com/locate/saa

Synthesis, photoluminescent behaviors, and theoretical studies of two novel ketocoumarin derivatives

Jing Li, Xianggao Li*, Shirong Wang

School of Chemical Engineering and Technology, Tianjin University, Tianjin 300072, China

ARTICLE INFO

Article history:
Received 29 August 2011
Received in revised form
13 November 2011
Accepted 18 November 2011

Keywords:
Coumarin
Synthesis
UV–vis
Photoluminescence
DFT studies

ABSTRACT

Two new coumarin derivatives, 3-[3-(4-formylphenyl)prop-2-enoyl]-coumarin (FEC) and 4-hydroxy-3-[3-(4-formylphenyl)prop-2-enoyl]-coumarin (HFEC), were synthesized and characterized by MS, ^{1}H NMR, FT-IR, and TG. The UV–vis absorption and photoluminescence (PL) of FEC and HFEC were also studied. Results show that the two compounds exhibit high fluorescence quantum yields, large Stokes shifts, and strong blue emissions. The molecular structures, the lowest energy transitions, the resonance frequencies, and the UV–vis spectra of FEC and HFEC were calculated using the density functional theory (DFT) and time-dependent density functional theory (TD-DFT) at the B3LYP/6-31G(d) level.

1. Introduction

Coumarin and its derivatives have received considerable attention in the past few years not only for their versatile biological and medical properties [1], such as antioxidant [2], anti-inflammatory [3], antibacterial [4], and anticancer activities [5], but also for their sufficient fluorescence in the visible light range [6], large Stokes shifts [7], and high quantum yields [8], among others. In addition, their photochemical and photophysical properties can be readily modified by the introduction of substituents in the coumarin ring, affording more flexibility that fit well in various applications. For example, recent research suggests that the fusion of a chalcone moiety to the coumarin ring is quite promising for the synthesis of derivatives with an extended spectral range (270–600 nm for the absorption band and 400–700 nm for the emission band) [6,9] and produce substances that can be used as blue, green, and red dopants in organic light-emitting diodes (OLEDs). Many ketocoumarin-based electroluminescent (EL) materials have been and are currently being developed [10–12].

In the current work, we report the synthesis, photophysical property, and theoretical investigation of two novel ketocoumarin derivatives, 3-[3-(4-formylphenyl)prop-2-enoyl]-coumarin (FEC) and 4-hydroxy-3-[3-(4-formylphenyl)prop-2-enoyl]-coumarin (HFEC). These derivatives exhibit strong blue emissions under ultraviolet light excitation. HFEC has an additional hydroxyl group at the 4-position of the coumarin ring compared with FEC. The main purpose of the current investigation is to understand the effect of substituents in the coumarin skeleton on the photoluminescent properties of coumarin.

2. Experimental

2.1. Materials and methods

IR spectra (400–4000 cm^{-1}) were measured on a Nicolet 380 spectrophotometer. ^{1}H NMR spectra were obtained using a Varian Inova 500 spectrometer (at 500 MHz). Mass spectra were recorded on a micrOTOF-Q II mass spectrometer. Melting points were taken using a RY-1 micro melting apparatus; the thermometer was uncorrected. Thermogravimetric (TG) analysis was carried out on a Q500 thermal analysis instrument. UV–vis absorption and emission spectra were recorded using a Thermo Evolution 300 spectrometer and a Cary Eclipse spectrometer, respectively. All the chemicals were commercially available and used without further purification. All the solvents were dried using standard methods before use.

2.2. Synthesis and characterization of FEC and HFEC

The synthetic routes are shown in Scheme 1.

2.2.1. 3-Acetyl-coumarin (1)

Salicylaldehyde (10.6 mL, 0.1 mol), ethyl acetoacetate (12.6 mL, 0.1 mol), piperidine (2 mL), and ethanol (200 mL) were all placed into a 500 mL round-bottomed flask. The resulting mixture was

* Corresponding author. Tel.: +86 22 27404208; fax: +86 22 27892279.
E-mail address: lixianggao@hotmail.com (X. Li).

1386-1425/$ – see front matter © 2011 Elsevier B.V. All rights reserved.
doi:10.1016/j.saa.2011.11.044

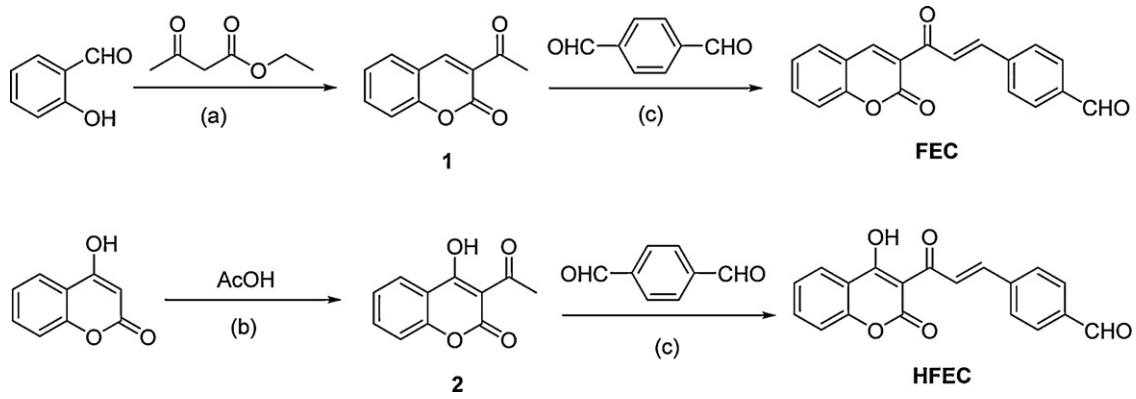

Scheme 1. Synthetic routes to FEC and HFEC.

heated to reflux under magnetic stirring for 4 h, after which the solution was cooled to room temperature and the separated yellowish solid was filtered off. This was subsequently recrystallized from ethanol to obtain the compound 1 (15.2 g, 80.6%). m.p. 121–122 °C. ^{1}H NMR ($CDCl_3$, δ, ppm): 2.732 (s, 3H, CH_3), 7.333–7.679 (m, 4H, Aryl-H), 8.517 (s, 1H, 4-H).

2.2.2. 3-Acetyl-4-hydroxy-coumarin (2)

Phosphorus oxychloride (25 mL, 0.1 mol) was added to a solution of 4-hydroxycoumarin (16.2 g, 0.1 mol) in glacial acetic acid (90 mL, 1.4 mol). The mixture was heated at reflux for 1 h. After cooling, the precipitate was collected and recrystallized from ethanol to obtain compound 2 as white needles (15.3 g, 70.5%). m.p. 139–140 °C. ^{1}H NMR ($CDCl_3$, δ, ppm): 2.790 (s, 3H, CH_3), 7.265–8.078 (m, 4H, Aryl-H).

2.2.3. FEC

A mixture of compound 1 (18.8 g, 0.1 mol), benzene-1,4-dicarboxaldehyde (26.8 g, 0.2 mol), and piperidine (3 mL) in glacial acetic acid (200 mL) was refluxed for 5 h and then cooled to room temperature. Afterwards, the precipitate was filtered and dried. The crude product was recrystallized from an ethanol/acetonitrile (v:v = 1:1) mixture solvent to produce the pure product of FEC (22.8 g, 75.1%). m.p. 204–205 °C. IR (KBr pellet cm^{-1}): 3040 (aryl-CH), 1720 (C=O, lactone), 1690 (C=O, formyl), 1670 (C=O), 1560 (C=C), 984 (C–O–C) cm^{-1}. ^{1}H NMR ($CDCl_3$, δ, ppm): 10.049 (s, 1H), 8.631 (s, 1H), 8.078 (d, J = 16.0 Hz, 1H), 7.927 (d, J = 8.0 Hz, 2H), 7.871 (d, J = 15.5 Hz, 1H), 7.826 (d, J = 8.0 Hz, 2H), 7.686 (q, J = 13.3 Hz, 2H), 7.394 (m, 2H). HRMS (ESI$^+$): m/z: calcd for $C_{19}H_{12}O_4$: 327.0628 [M+Na$^+$]; found: 327.0627.

2.2.4. HFEC

The preparation of HFEC was similar to that described for FEC. The yield of the corresponding synthesis reaction was 80.1%. m.p. 209–210 °C. IR (KBr pellet cm^{-1}): 3040 (aryl-CH), 1730 (C=O, lactone), 1700 (C=O, formyl), 1630 (C=O), 1540 (C=C), 982 (C–O–C) cm^{-1}. ^{1}H NMR ($CDCl_3$, δ, ppm): 10.060 (s, 1H), 8.544 (d, J = 15.5 Hz, 1H), 8.108 (q, J = 7.8 Hz, 1H), 8.037 (d, J = 16.0 Hz, 1H), 7.947 (d, J = 8.0 Hz, 2H), 7.866 (d, J = 8.0 Hz, 2H), 7.720 (m, 1H), 7.350 (m, 2H). HRMS (ESI$^+$): m/z: calcd for $C_{19}H_{12}O_5$: 343.0577 [M+Na$^+$]; found: 343.0552.

2.3. Quantum chemical calculations

The structures of FEC and HFEC were optimized by the semiempirical density functional theory (DFT) using a B3LYP/6-31G(d) [13] basis set. The structural energies and resonance frequencies of FEC and HFEC were calculated at the B3LYP/6-31G(d) level. The solvent polarity effects were included by the polarizable continuum model (PCM) [14]. The structure optimization and the energy and frequency calculations were performed using the GAUSSIAN 03 program [15].

3. Results and discussion

3.1. Synthesis

Compound 1, compound 2, FEC, and HFEC were all prepared according to the method described earlier [16–18]. Knoevenagel condensation of salicylaldehyde with ethyl acetoacetate yielded compound 1. For the acetylation of 4-hydroxycoumarin to yield compound 2, glacial acetic acid was used as acetylating agent in the presence of $POCl_3$. The Claisen–Schmidt condensation of compounds 1 and 2 with benzene-1,4-dicarboxaldehyde yielded the coumarin–chalcones FEC and HFEC, respectively.

The structure and purity of the resulting new compounds (i.e., FEC and HFEC) were confirmed by spectral data. In the IR spectra of the two compounds, the strong bands at around 1720 and 1730 cm^{-1}, respectively, confirm the presence of a coumarin skeleton. Note that for HFEC, no ν_{-OH} of the hydroxyl group appears in its IR spectrum. This is due to the existence of a strong intra-molecular hydrogen bond between the hydroxyl group and the ketonic oxygen in its structure [16].

The structures of FEC and HFEC were also confirmed by ^{1}H NMR spectroscopy. The ^{1}H NMR spectra of FEC show a clearly distinguishable intense singlet at δ = 8.631 ppm for H-4 of the coumarin nucleus. Such a signal characterizes coumarin system protons [12]. Moreover, for FEC and HFEC, characteristic formyl proton singlets at δ = 10.049 and 10.060 ppm, respectively, are apparent in the ^{1}H NMR spectra.

3.2. Thermal properties of FEC and HFEC

In order to investigate the thermal stabilities of FEC and HFEC, the TG experiments were carried out in the temperature range of 30–800 °C and a heating rate of 10° min^{-1} in nitrogen atmosphere. The resulting thermograph is shown in Fig. 1. The TG curves for FEC and HFEC show a clear plateau, followed by a sharp decomposition curve. The loss in weight of the two compounds is rapid when heated above 246 °C. These results indicate that FEC and HFEC are stable up to 246 °C, after which they decompose rapidly and completely at a temperature above 363 °C. This finding confirms that the two compounds have similar and excellent thermal stabilities.

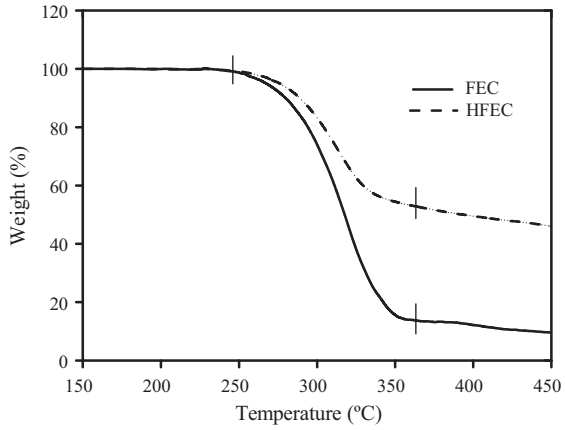

Fig. 1. TG curves of FEC and HFEC.

Table 1
UV–vis absorption and fluorescence spectra data for compounds 1 and 2, FEC, and HFEC.

Compound	$\lambda_{a,max}$ (nm)	$\lambda_{e,max}$ (nm)	Stake's shift (nm)
Compound 1	300, 341	438	97
Compound 2	300, 324	402	78
FEC	333	460	127
HFEC	370	480	110

3.3. *UV–vis absorption and fluorescence of compounds 1 and 2, FEC, and HFEC*

UV–vis absorption and photoluminescence spectra of compounds 1 and 2, FEC, and HFEC in dilute dichloromethane solutions are given in Figs. 2 and 3, respectively, and the relevant data are listed in Table 1. Compound 1 shows a sharp absorption peak at 300 nm, with a shoulder at 341 nm. Compound 2 shows a sharp absorption peak at 300 nm, with a shoulder at 324 nm. The spectral shape of compound 2 is similar to that of compound 1 because of their highly similar structures. However, the shoulder peak at 324 nm of compound 2 is blue-shifted compared with that of compound 1 (341 nm). It has been suggested that compound 2 has an intra-molecular hydrogen bond between the hydroxyl group and the ketonic oxygen in its chemical structure, thus weakening the electron-withdrawing effect of the 3-acetyl group.

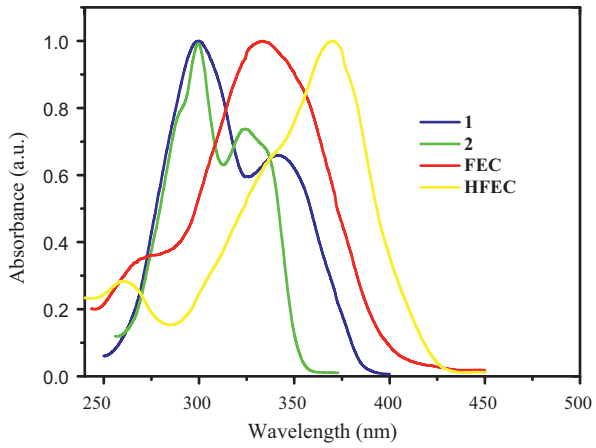

Fig. 2. UV–vis absorption spectra of compound 1, compound 2, FEC, and HFEC in dichloromethane at room temperature ($C = 5.00 \times 10^{-5}$ mol/L). (For interpretation of the references to color in this figure legend, the reader is referred to the web version of the article.)

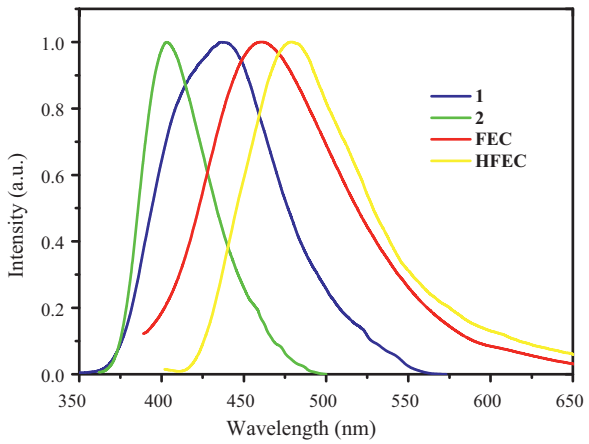

Fig. 3. Fluorescence emission spectra of compound 1(λ_{ex} = 341 nm), compound 2(λ_{ex} = 324 nm), FEC(λ_{ex} = 333 nm), and HFEC(λ_{ex} = 370 nm) in dichloromethane at room temperature ($C = 5.00 \times 10^{-5}$ mol/L). (For interpretation of the references to color in this figure legend, the reader is referred to the web version of the article.)

FEC and HFEC exhibit absorption spectral features that are quite different from those of the corresponding starting compounds, i.e., compound 1 and compound 2, respectively. FEC and HFEC each have only one intense absorption peak at 333 and 370 nm, respectively. Due to the elongated conjugation in the FEC structure, the absorption peak of the compound is red-shifted compared with that of compound 1 at 300 nm. Similarly, the absorption peak of HFEC is red-shifted compared with the sharp absorption peak of compound 2. Note that the absorption peak of HFEC is red-shifted by 37 nm with respect to that of FEC. FEC and HFEC are typical intramolecular charge transfer compounds. Their molecules consist of a typical D–π–A structure, in which 3-carbonylcoumarinyl, styryl and formyl groups are employed as donor (D), π-conjugated center (π) and acceptor (A) moieties, respectively. Thus, the reason for the difference between the absorption features of FEC and HFEC may be attributed to the increase of the electron-donating capability of the 3-carbonylcoumarinyl group and the greater strength of the intra-molecular charge transfer upon the introduction of a hydroxyl group to the 4-position of the coumarin ring.

The emission peak of compound 2 appears at around 402 nm, which is blue-shifted by about 36 nm with respect to that of compound 1 at 438 nm, due to the existence of the intermolecular hydrogen bond in the structure of compound 2. In addition, the emission peaks of FEC and HFEC appear at around 460 and 480 nm, respectively; they are bathochromically shifted with respect to those of the corresponding compounds, compound 1, and compound 2. The emission peak of HFEC is red-shifted by about 20 nm with respect to that of FEC, because of an electron repelling hydroxyl group in the 4-position of the coumarin ring.

In Figs. 2 and 3, for FEC and HFEC, respectively, the Stokes shifts between the absorption and the emission maximum are significant. The efficient π-conjugation in the molecule is known to be responsible for the charge-transfer nature of the emissive excited state and for the observed relatively large Stokes shifts.

The 3-carbonylcoumarinyl group of the styrene-modified ketocoumarins can also be used as an acceptor moiety. In FEC, for example, when the *p*-formylphenyl moiety is replaced with a *p*-N,N-diphenylaminophenyl group, the maximum absorption peak is red-shifted to 465 nm because of the elongated conjugation in its structure. However, the maximum emission peak is blue-shifted to 430 nm [9] because the 3-carbonylcoumarinyl group acts as an acceptor moiety, and the entire molecule adopts a typical A–π–D structure, which leads to the reversal of the intramolecular charge-transfer route.

Table 2
Mulliken charges (e) of FEC and HFEC obtained by the B3LYP/6-31G(d) method.

Molecules	O(C–O–C)	O((O)=C–O)	O(C=O)	O(O=C–H)
FEC/HFEC	−0.519/−0.519	−0.436/−0.476	−0.440/−0.455	−0.400/−0.403

3.4. Fluorescence quantum yields of the compounds ($\Phi_{S,FEC}$ and $\Phi_{S,HFEC}$)

The fluorescence quantum yields of FEC and HFEC in dichloromethane solutions can be estimated from the following equation [19]:

$$\Phi_S = \Phi_R \cdot \frac{A_R}{F_R} \cdot \frac{F_S}{A_S} \left(\frac{n_S}{n_R}\right)^2$$

where Φ_R is the quantum yield of the standard, A is the absorbance at the wavelength of the excitation, F is the integrated intensity of the emission spectra, n is the refractive index of the solution, index (S) denotes the sample, and (R) denotes the reference. The standard fluorophore for the quantum yield measurements is quinine sulphate in 0.2 mol dm^{-3} H_2SO_4 (Φ_R = 0.51) [20]. In the current research, the Φ_S of FEC and HFEC are 0.55 and 0.70, respectively. The typical D–π–A structure in the two compounds leads to a high fluorescence quantum yield. Compared with $\Phi_{S,FEC}$, $\Phi_{S,HFEC}$ increased due to the presence of the hydroxyl group, enhancing the electron density of the coumarin ring.

Table 3
The comparison of λ_{max} (nm) obtained by calculation and experiment.

Compound	Calc.[a]		Exp.[b]
	Without solvent	Dichloromethane	
FEC	320 (0.8553)	334 (0.8239)	333
HFEC	360 (0.8225)	372 (0.8521)	370

[a] Calculated oscillator strengths are given in parenthesis.
[b] Solvent is dichloromethane.

3.5. Quantum chemical calculations

To obtain further insight into the geometrical configuration and photophysical properties of FEC and HFEC, DFT calculations were performed at the B3LYP/6-31G(d) level for geometry optimization. The optimized structures and electron distribution of the HOMO and LUMO of FEC and HFEC are shown in Fig. 4.

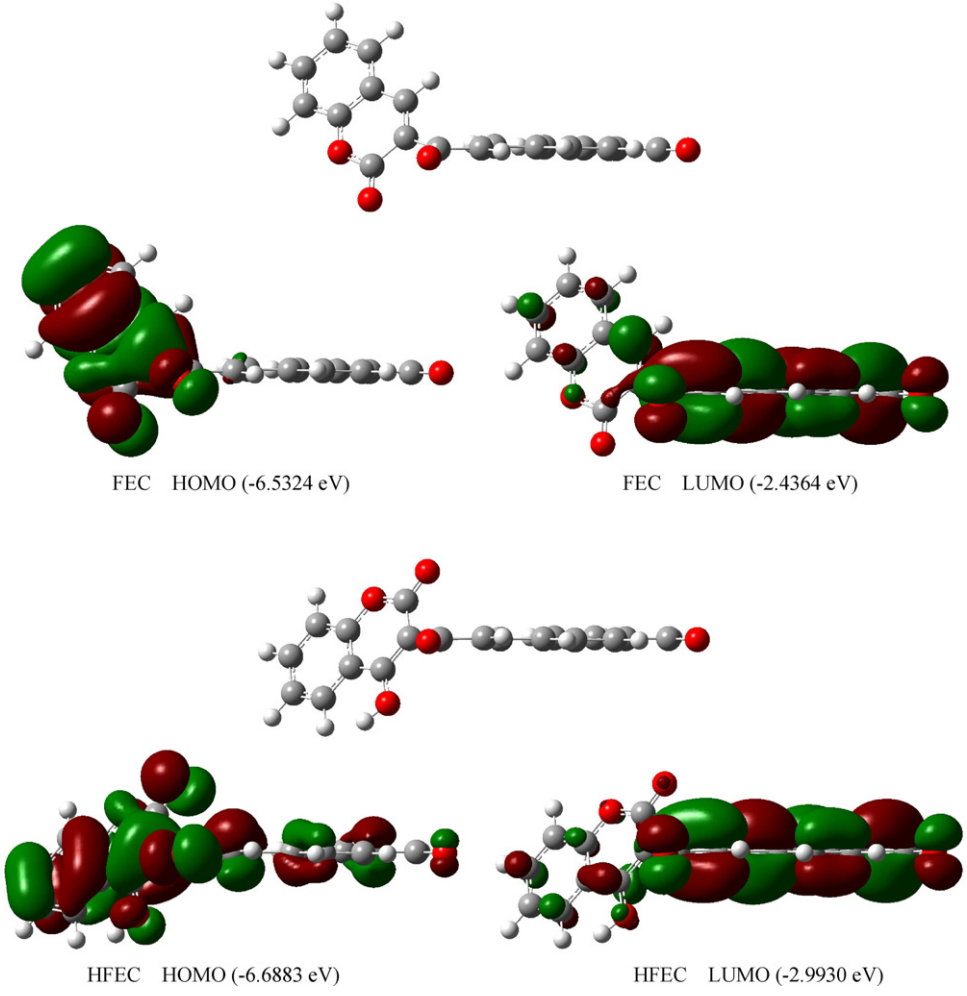

Fig. 4. Optimized structures and HOMO and LUMO electron distributions of FEC and HFEC.

Table 4
Comparison of the calculated and experimental infrared data of FEC and HFEC.

No.	Exp. (FEC/HFEC)		Calcd. (FEC/HFEC)			Vibratory feature
	Freq.[a]	Int. (IR)[b]	Non scaled	Scaled[c]	Int. (IR)	
1	3040/3040	w/w	3181/3166	3058/3044	11.92/14.85	$\nu_{=CH}$
2	2820/2820	m/m	2915/2912	2803/2799	165.74/173.41	$\nu_{=CH}$(CHO)
3	1720/1730	v/v	1839/1827	1768/1756	514.70/536.41	$\nu_{C=O}$(COO)
4	1690/1700	v/v	1799/1797	1729/1728	305.39/315.57	$\nu_{C=O}$(CHO)
5	1670/1630	s/s	1742/1747	1675/1680	196.95/364.04	$\nu_{C=O}$(CO)
6	1610/1600	v/v	1673/1684	1608/1619	120.46/220.80	$\nu_{C=C}$
7	1560/1540	s/v	1614/1618	1552/1556	83.06/104.58	$\nu_{C=C}$(CH=CH)
8	1180/1200	s/s	1232/1267	1184/1218	256.22/176.13	$\nu_{C=C}$
9	984/982	s/s	994/982	956/944	130.07/177.22	ν_{C-O-C}
10	822/829	m/m	863/870	830/836	56.70/32.10	$\delta_{=CH}$
11	752/764	m/m	774/761	744/732	64.22/82.00	$\delta_{=CH}$
12	577/588	m/m	594/580	571/557	30.03/23.15	$\delta_{=CH}$

[a] Frequencies in cm^{-1}.
[b] m: middle, s: strong, v: very strong, w: weak.
[c] Scaling factor using 0.9613.

The chalcone skeleton is essentially planar, which is rotated significantly out of the plane of the coumarin ring. This nonplanar geometry structure can effectively prevent the aggregation of molecules, causing FEC and HFEC to exhibit high fluorescence quantum yields, as presented in Section 3.4. The HOMO and LUMO levels of FEC are −6.5324 and −2.4364 eV, respectively, and the energy gap between HOMO and LUMO is about 4.0960 eV. The corresponding levels for HFEC are −6.6883 and −2.9930 eV, and the relative energy gap is 3.6953 eV. The large HOMO–LUMO gaps of FEC and HFEC demonstrate their high kinetic stabilities and low chemical reactivities, given that the addition of electrons to a high-lying LUMO or their extraction from a low-lying HOMO is energetically unfavorable [21]. For FEC and HFEC, the HOMO is located in the electron-donating group and in the whole molecular skeleton, respectively. For both FEC and HFEC, the LUMO is located in the electron-withdrawing group through the π-spacer. Consequently, the transition from HOMO to LUMO is easier in HFEC than in FEC. This causes the value of the energy gap of HFEC to be lower than that of FEC. In turn, this leads to the absorption peak of HFEC to be bathochromically shifted compared with that of FEC, as shown in Section 3.3.

Mulliken charges of FEC and HFEC were also obtained, and the charges of oxygen atoms are listed in Table 2. Introducing a hydroxyl group to the 4-position of the coumarin ring results in the increase in the negative charges in the electron-attracting oxygen atoms, especially in the lactone carbonyl oxygen atom. This is due to the electron-repelling effect of the hydroxyl group conjugating with the coumarin ring.

The UV–vis absorption spectra of FEC and HFEC were also calculated by the time-dependent density functional theory (TD-DFT) at the same level. The max absorption wavelengths correspond to the S1 state. Table 3 lists the experimental and calculated λ_{max} (nm) values of the corresponding UV–vis absorption spectra for the S1 states of FEC and HFEC. Solvent effects were considered in the PCM model, and the discrepancy between the theoretical and experimental λ_{max} is reduced from 13 nm to 1 nm for FEC and from 10 nm to 2 nm for HFEC. These results show the remarkable increase in accuracy and are in very good agreement with the experimental measurements when the solvent effects are taken into account.

The resonance frequency calculations of FEC and HFEC were carried out at the B3LYP/6-31G(d) level to study the IR spectra of the two structures. The calculation of resonance frequency is extensively used in organic chemistry for the identification of functional groups of organic compounds and for the study of molecular conformations, reaction kinetics, etc. The observed and calculated data of the IR spectra of FEC and HFEC are given in Table 4. The value of the calculated IR spectrum is slightly higher than the experimental value, which may be due to the fact that the result obtained by the calculation is the harmonic oscillator frequency and that the experimental value also contains the an harmonic oscillator frequency. In addition, data of the IR spectra were modified using 0.9613 [22] as the frequency scaling factor. The resulting consistent relation graph between the calculated and experimental data of FEC and HFEC are shown in Fig. 5. The linear slope and intercept of FEC are 1.0467 and −5.4282 for the non-scaled data, and 1.0063 and −5.2663 for the scaled data, respectively. For HFEC, the corresponding non-scaled data are 1.0473 and −5.1105, and the

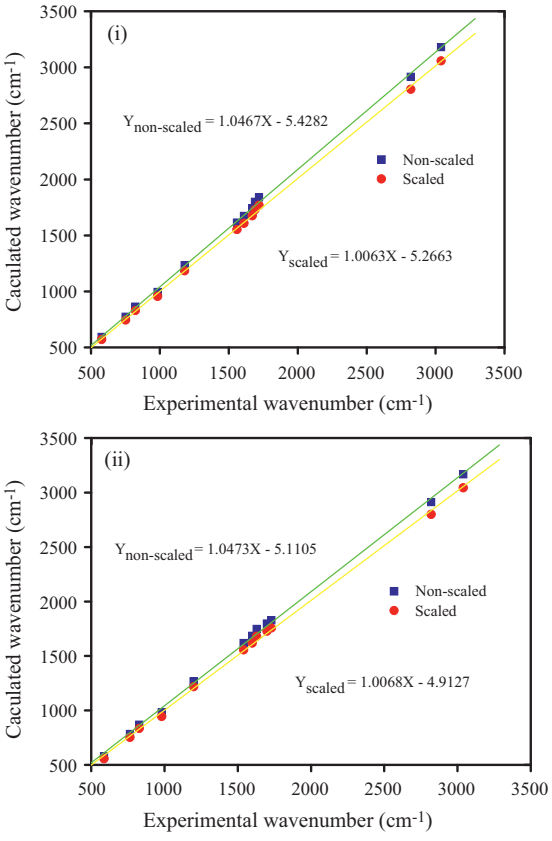

Fig. 5. Consistency of the wavenumbers of the calculated and experimental IR spectra main peaks of FEC (I) and HFEC (II).

relative scaled data are 1.0068 and −4.9127, respectively. These results indicate that the description error clearly decreases after the introduction of the frequency-scaling factor, and the calculated data are in good agreement with the experimental value.

4. Conclusions

Two novel ketocoumarin derivatives, FEC and HFEC, have been successfully synthesized. Their photophysical properties have also been investigated. Both of them have excellent thermal stabilities, exhibit high fluorescence quantum yields, bright blue emissions (460 and 480 nm) and large Stokes shifts. At the same time, the HOMO–LUMO levels and the IR and UV–vis spectra of FEC and HFEC have been studied with the DFT and TD-DFT at the B3LYP/6-31G(d) level. The results demonstrate that the calculation outcomes are in good agreement with the experimental data. Based on the results, FEC and HFEC are potential candidates for use in opto- or opto-electronic blue-emitting devices. Their other characteristics will be studied in the future.

Acknowledgement

This work was financially supported by National Natural Science Foundation of China (21176180).

References

[1] M.E. Riveiro, D. Maes, R. Vázquez, M. Vermeulen, S. Mangelinckx, J. Jacobs, S. Debenedetti, C. Shayo, N. De Kimpe, C. Davio, Bioorg. Med. Chem. 17 (2009) 6547.
[2] M. Mladenović, M. Mihailović, D. Bogojević, S. Matić, N. Nićiforović, V. Mihailović, N. Vuković, S. Sukdolak, S. Solujić, Int. J. Mol. Sci. 12 (2011) 2822.
[3] Y.F. Ma, J.Y. Jung, Y.J. Jung, J.H. Choi, W.S. Jeong, Y.S. Song, J.S. Kang, K. Bi, M.J. Kim, J. Food Sci. Nutr. 14 (2009) 179.
[4] N. Hamdi, V. Passarelli, A. Romerosa, C. R. Chimie 14 (2011) 548.
[5] M.E. Riveiro, N. De Kimpe, A. Moglioni, R. Vazquez, F. Monczor, C. Shayo, C. Davio, Curr. Med. Chem. 17 (2010) 1325.
[6] A.R. Jagtap, V.S. Satam, R.N. Rajule, V.R. Kanetkar, Dyes Pigments 91 (2011) 20.
[7] H. Zhang, T.Z. Yu, Y.L. Zhao, D.W. Fan, Y.J. Xia, P. Zhang, Synth. Met. 160 (2010) 1642.
[8] D. Ray, P.K. Bharadwaj, Inorg. Chem. 47 (2008) 2252.
[9] Y.F. Sun, Y.P. Cui, Dyes Pigments 78 (2008) 65.
[10] X. Li, Y.X. Zhao, T. Wang, M.Q. Shi, F.P. Wu, Dyes Pigments 74 (2007) 108.
[11] Z.L. Huang, N. Li, Y.F. Sun, H.Z. Wang, H.C. Song, Z.L. Xu, J. Mol. Struct. 657 (2003) 343.
[12] Y.F. Sun, S.H. Xu, R.T. Wu, Z.Y. Wang, Z.B. Zheng, J.K. Li, Y.P. Cui, Dyes Pigments 87 (2010) 109.
[13] R. Ditchfield, W.J. Hehre, J.A. Pople, J. Chem. Phys. 54 (1971) 724.
[14] J. Tomasi, M. Persico, Chem. Rev. 94 (1994) 2027.
[15] M.J. Frisch, G.W. Trucks, H.B. Schlegel, G.E. Scuseria, M.A. Robb, J.R. Cheeseman, J.A. Montgomery Jr., T. Vreven, K.N. Kudin, J.C. Burant, J.M. Millam, S.S. Iyengar, J. Tomasi, V. Barone, B. Mennucci, M. Cossi, G. Scalmani, N. Rega, G.A. Petersson, H. Nakatsuji, M. Hada, M. Ehara, K. Toyota, R. Fukuda, J. Hasegawa, M. Ishida, T. Nakajima, Y. Honda, O. Kitao, H. Nakai, M. Klene, X. Li, J.E. Knox, H.P. Hratchian, J.B. Cross, V. Bakken, C. Adamo, J. Jaramillo, R. Gomperts, R.E. Stratmann, O. Yazyev, A.J. Austin, R. Cammi, C. Pomelli, J.W. Ochterski, P.Y. Ayala, K. Morokuma, G.A. Voth, P. Salvador, J.J. Dannenberg, V.G. Zakrzewski, S. Dapprich, A.D. Daniels, M.C. Strain, O. Farkas, D.K. Malick, A.D. Rabuck, K. Raghavachari, J.B. Foresman, J.V. Ortiz, Q. Cui, A.G. Baboul, S. Clifford, J. Cioslowski, B.B. Stefanov, G. Liu, A. Liashenko, P. Piskorz, I. Komaromi, R.L. Martin, D.J. Fox, T. Keith, M.A. Al-Laham, C.Y. Peng, A. Nanayakkara, M. Challacombe, P.M.W. Gill, B. Johnson, W. Chen, M.W. Wong, C. Gonzalez, J.A. Pople, GAUSSIAN 03, Revision D.1, Gaussian, Inc., Wallingford, CT, 2005.
[16] N. Hamdi, C. Fischmeister, M.C. Puerta, P. Valerga, Med. Chem. Res. 20 (2011) 522.
[17] S. Khode, V. Maddi, P. Aragade, M. Palkar, P.K. Ronad, S. Mamledesai, A.H.M. Thippeswamy, D. Satyanarayana, Eur. J. Med. Chem. 44 (2009) 1682.
[18] O.M. Abdelhafez, K.M. Amin, R.Z. Batran, T.J. Maher, S.A. Nada, S. Sethumadhavan, Bioorg. Med. Chem. 18 (2010) 3371.
[19] A. Huczyński, I. Paluch, M. Ratajczak-Sitarz, A. Katrusiak, J. Stefańska, B. Brzezinski, F. Bartl, J. Mol. Struct. 891 (2008) 481.
[20] S.R. Meech, D. Phillips, J. Photochem. 23 (1983) 193.
[21] H. Zhang, T.Z Yu, Y.L. Zhao, D.W Fan, Y.J. Xia, P. Zhang, Y.Q. Qiu, L.L. Chen, Spectrochim. Acta A 75 (2010) 325.
[22] Y.L. Fu, W. Huang, C.L. Li, L.Y. Wang, Y.S. Wei, Y. Huang, X.H. Zhang, Z.Y. Wen, Z.X. Zhang, Dyes Pigments 82 (2009) 409.